SUPPLEMENTARY MATERIAL

$FeCu_3$-LDH/MoS_2 superlattice-modified carbon paper as the integrated sensor for the sensitive detection of nitrofurantoin in various samples

Xueting Wang[a], Yuehua Li[a, *], Boran Tong[a], Xingwen Wang[a, b, *], Wei Meng[a], Jing Zhang[a] and Chao Han[a, *]

[a] College of Chemical Engineering, North China University of Science and Technology, Tangshan, 063210, China

[b] North China University of Science and Technology Affiliated Hospital, Tangshan, Hebei 063009, China

Communication to: Analytical Methods

---

*To whom correspondence should be addressed.

Email: hanchao@ncst.edu.cn (C.Han); mengwei@ncst.edu.cn (W. Meng); tsliyuehua@126.com; starwin1011@163.com

Catalogue

1. Materials and reagents

Thiourea (99.0%), $Fe(NO_3)_2 \cdot 9H_2O$ (99.0%), Na_2SO_4, KNO_3, $NaH_2PO_4 \cdot 2H_2O$ (99.0%), $Na_2HPO_4 \cdot 12H_2O$ (99.0%), O-nitrophenol, M-nitrophenol, and P-nitrophenol were provided by Beijing J&K Co., Ltd. Nitrofurantoin (NFT), Ascorbic acid, Dopamine, Ammonium molybdate (99.0%), $Ni(NO_3)_2 \cdot 6H_2O$ (99.0%), $Co(NO_3)_2 \cdot 6H_2O$ (99.0%), N, N-dimethylformamide (DMF, 99.0%), were obtained from Aladdin. Urea (AR), Citric acid, Absolute ethanol (99.7%) were purchased from Yongda Chemical Reagent Co., Ltd. Hexamethylenetetramine, Nafion (5*wt*%) were achieved from Shanghai Debo Biotechnology Co., Ltd. $Cu(NO_3)_2 \cdot 3H_2O$ (99.0%), Metronidazole, Ornidazole were acquired from McLean Biochemical Technology Co., Ltd. All chemicals were used directly without any purification treatment. In addition, carbon paper (CP) was acquired from Shanghai Hesen Electric Co., Ltd. All reagents were used without further purification. The real sample of Normal human serum and nitrofurantoin enteric-coated tablets were purchased through the commercial channels. The serum was purchased from Beijing Solarbio Science & Technology Co., Ltd. The producer of nitrofurantoin enteric-coated tablets was Tianjin Lisheng Pharmaceutical Co., LTD. The sample of lake water was collected from the Jinghu in North China University of Science and Technology.

2. Materials equipment

The material composition of $FeCu_3$-LDH/MoS_2 (1:1) was investigated by X-ray diffraction (XRD) (D/MAX2500PC, Japan Rigaku Co., Ltd.) in the 2θ range of 5°~90° with an operating voltage and current of 40 kV and 40 mA. The size and morphology of $FeCu_3$-LDH/MoS_2 (1:1) were observed by scanning electron microscope (SEM) (JSM-IT100, Japan Electronics Co., Ltd.) and transmission electron microscope (TEM) (JEM-2100F, JEOL Ltd.). And energy dispersive spectroscopy (EDS) was used to determine the content and distribution of the elements contained in $FeCu_3$-LDH/MoS_2 (1:1). The elemental composition, chemical states and chemical bonding of $FeCu_3$-LDH/MoS_2 (1:1) were qualitatively analyzed by X-ray photoelectron spectroscopy (XPS).

3. Materials characterization

The electrochemical measurements were carried out on CHI660E electrochemical workstation with a standard three-electrode system consisting of $FeCu_3$-LDH/MoS_2/CP (1:1) as the working electrode, platinum electrode as auxiliary electrode and saturated calomel electrode as reference electrode. 0.1 M phosphate buffered saline (PBS) was prepared as the electrolyte solution.

The electrochemical activity area of the electrode materials was measured by cyclic voltammetry (CV) in solutions containing 0.1 M KCl and 5 mM $[Fe(CN)_6]^{3-/4-}$ at different scan rates (30~100 $mV \cdot s^{-1}$) under a potential window of -0.2~0.6 V. electrochemical impedance spectroscopy (EIS) was used to determine the impedance of the electrodes and to investigate the reaction mechanism of the electrode system and EIS was measured in the frequency range of $1 \sim 10^6$ Hz with an amplitude of 5 mV. The electrocatalytic performance of different electrode materials for NFT was investigated by CV in 0.1 M PBS with a voltage range of -1.0~0.2 V and a scan rate of 100 $mV \cdot s^{-1}$. The effect of scan rate (25~200 $mV \cdot s^{-1}$) and pH (5~9) on catalytic oxidation activities of NFT was also studied by CV method. Amperpmetric i-t curve (i-t) was used for quantitative analysis to obtain the detection range, sensitivity and detection limit of the sensor for NFT. In addition, the selectivity, reproducibility and stability of this electrochemical sensor were measured by i-t method, and actual sample detection of NFT in serum, lake water and nitrofurantoin enteric-coated tablets were also tested.

4. Correlation formula calculation

Interlayer spacing of $FeCu_3$-LDH with different anion intercalations were calculated according to the Bragg formula based on equation (1)[1].

$$2d\sin\theta = n\lambda \tag{1}$$

Where d is the layer spacing, θ is the diffraction angle, n is a positive integer, and λ is the wavelength of the incident wave of the X-ray diffractometer. For the same reflection, the relationship between $FeCu_3$-LDH-NO_3^- and $FeCu_3$-LDH-CO_3^{2-} layer spacing and diffraction angle satisfies formula (2)[1].

$$2d_1\sin\theta_1 = 2d_2\sin\theta_2 \tag{2}$$

According to the calibration curve of the redox reaction peak current and the square root of the scanning rate (Fig. 4a-c illustration), the electroactive area of the electrodes was calculated with the Randles-Sevcik equation based on equation (3)[2].

$$I_p = 2.69 \times 10^5 A D^{1/2} n^{3/2} v^{1/2} C \qquad (3)$$

Where I_p is the peak current (A), A is the electrochemically active area (cm^2), D is the diffusion coefficient (7.6×10^{-6} $cm^2\cdot s^{-1}$), n is the number of transferred electrons (n = 1 when 5 mM $[Fe(CN)_6]^{3-/4-}$), and v is the scanning rate ($V\cdot s^{-1}$). C is the concentration of redox reaction substance in solution ($mol\cdot cm^{-3}$).

The heterogeneous electron transfer rate (k_{et}) was calculated from equation (4)[3].

$$k_{et} = RT/n^2F^2AR_{ct}C \qquad (4)$$

Where R is the gas constant (8.314 $J\cdot mol^{-1}$), T is the room temperature (298.15 K), F is the Faraday constant (96485 $C\cdot mol^{-1}$), n is the number of transferred electrons (n = 1 at 5 mM $[Fe(CN)_6]^{3-/4-}$), and A is the electrode area (1.25 cm^2). C is the concentration of redox substances in the solution (5 mM).

5. SEM patterns

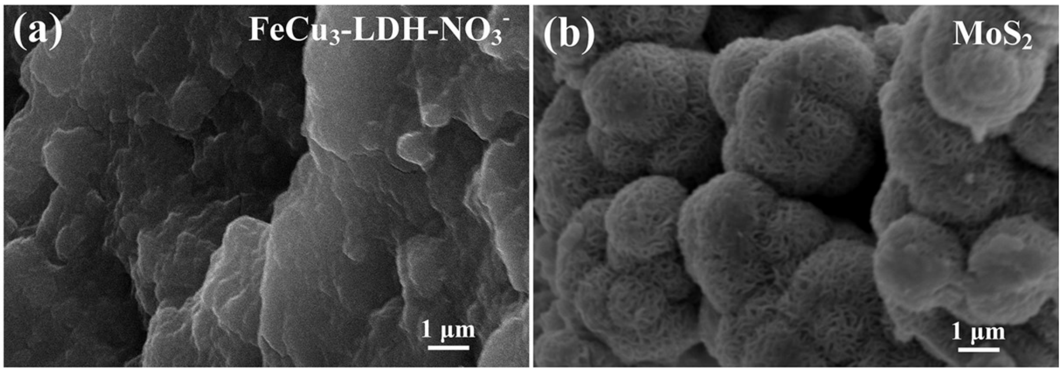

Fig. S1. (a, b) SEM images of $FeCu_3$-LDH-NO_3^-, MoS_2.

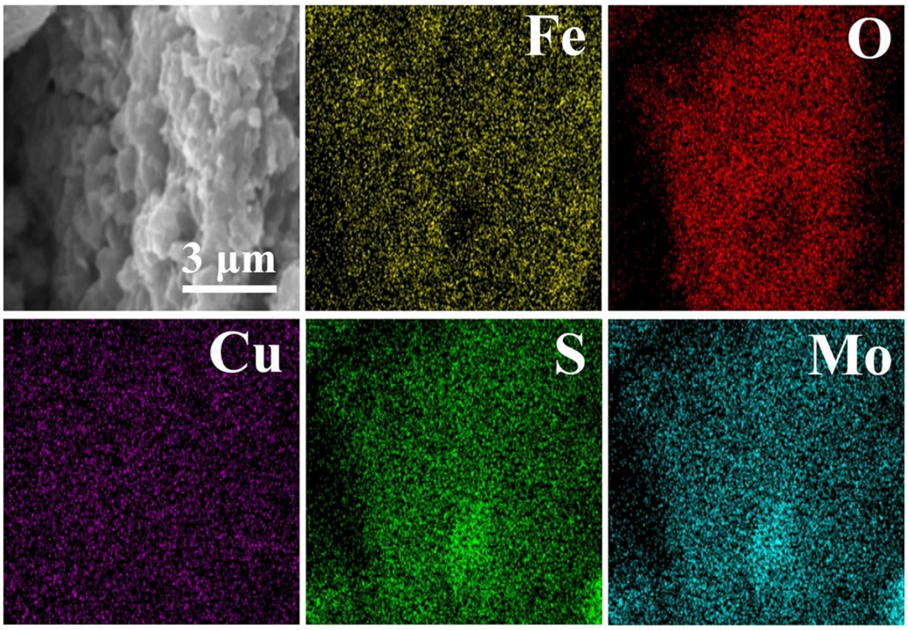

Fig. S2. EDS mapping of $FeCu_3$-LDH/MoS_2 (1:1).

6. X-ray photoelectron spectroscope

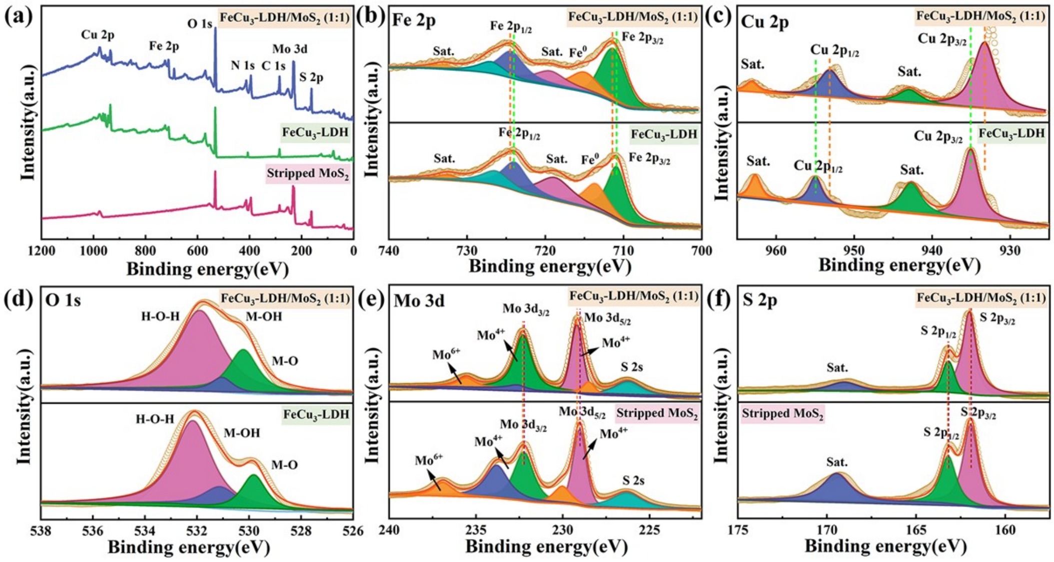

Fig. S3. (a) The full spectrum of FeCu$_3$-LDH/MoS$_2$ (1:1), FeCu$_3$-LDH and Stripped MoS$_2$. XPS high-resolution spectra of FeCu$_3$-LDH/MoS$_2$ (1:1), FeCu$_3$-LDH and MoS$_2$: (b) Fe 2p; (c) Cu 2p; (d) O 1s; (e) Mo 3d and S 2p.

7. Electrocatalytic behaviors of $FeCu_3$-LDH/MoS_2/CP with different mass ratio

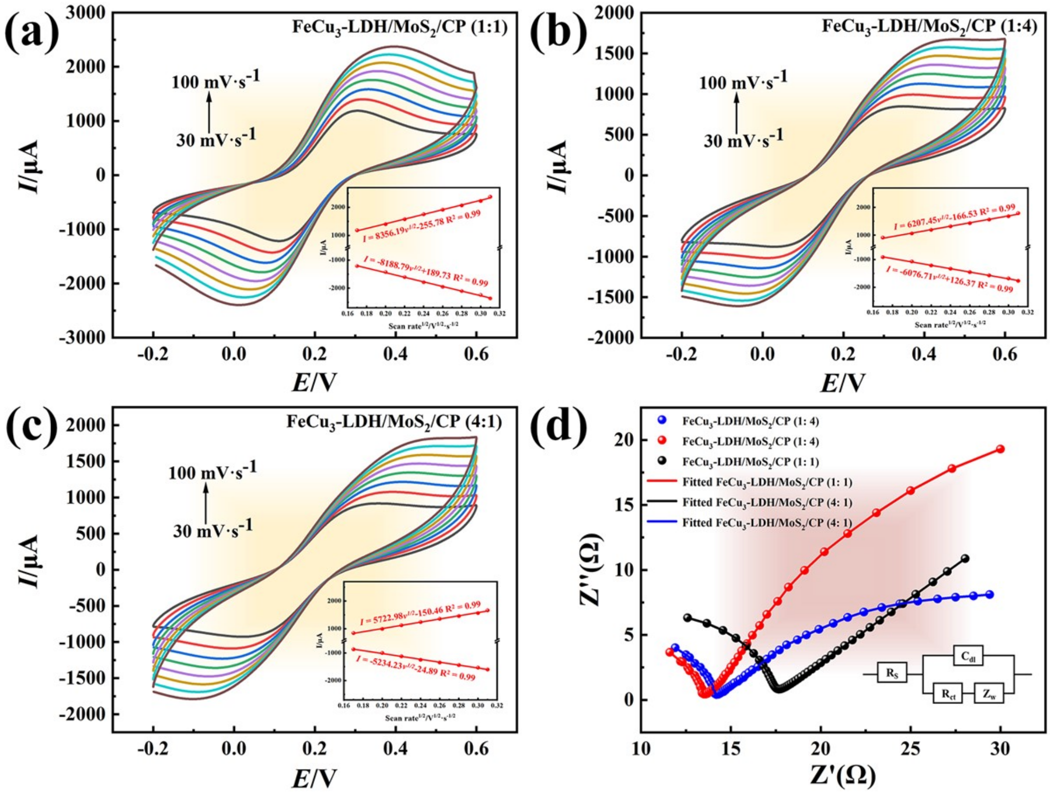

Fig. S4. CV curves of (a) $FeCu_3$-LDH/MoS_2/CP (1:1), (b) $FeCu_3$-LDH/MoS_2/CP (1:4) and (c) $FeCu_3$-LDH/MoS_2/CP (4:1) in 5.0 mM $[Fe (CN)_6]^{3-/4-}$ solution with 0.1 M KCl at increasing scanning velocities (30~100 mV·s^{-1}). Inset: corresponding plots of I_p vs. $v^{1/2}$; (d) EIS of $FeCu_3$-LDH/MoS_2/CP with different mass ratios. Inset: equivalent circuit diagram.

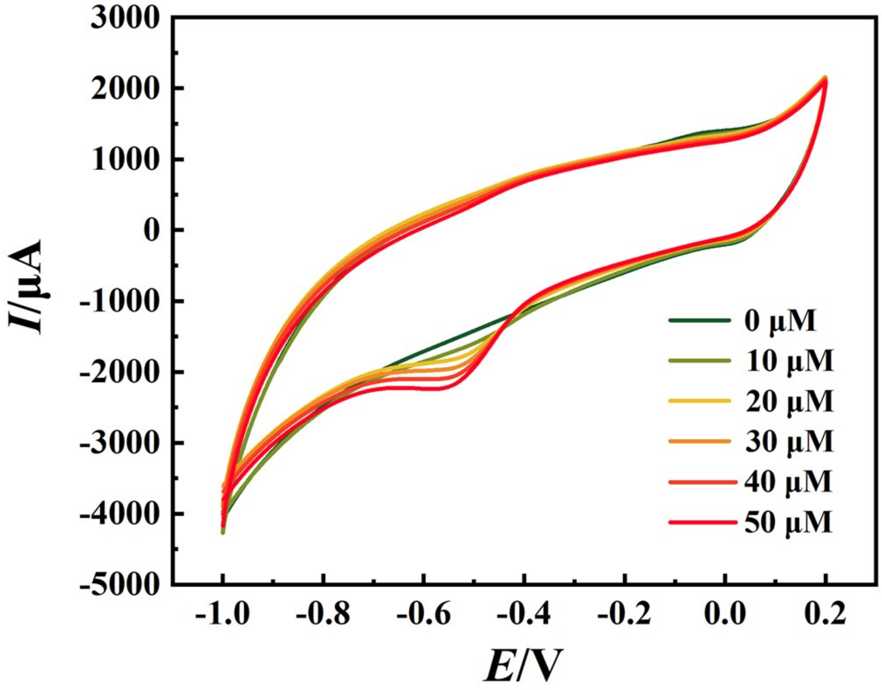

Fig. S5. CV curves of $FeCu_3$-LDH/MoS_2/CP (1:1) in the presence of NFT. Scan rates:100 mV·s^{-1}.

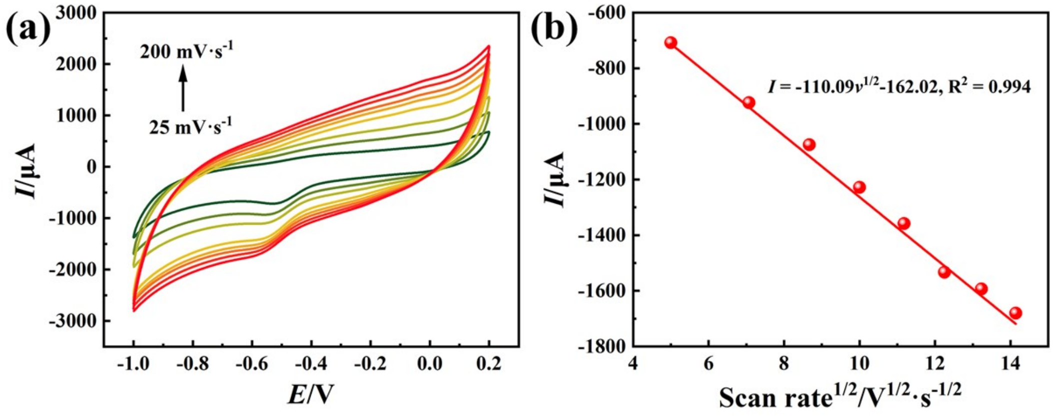

Fig. S6. The CV curves of FeCu$_3$-LDH/MoS$_2$/CP (1:1) in the presence of 50 μM NFT at different scan rates of 25~200 mV·s^{-1}; (b) Linear fitting plots of the redox peak current and the square root of scan rates.

8. The electrochemical mechanism of NFT

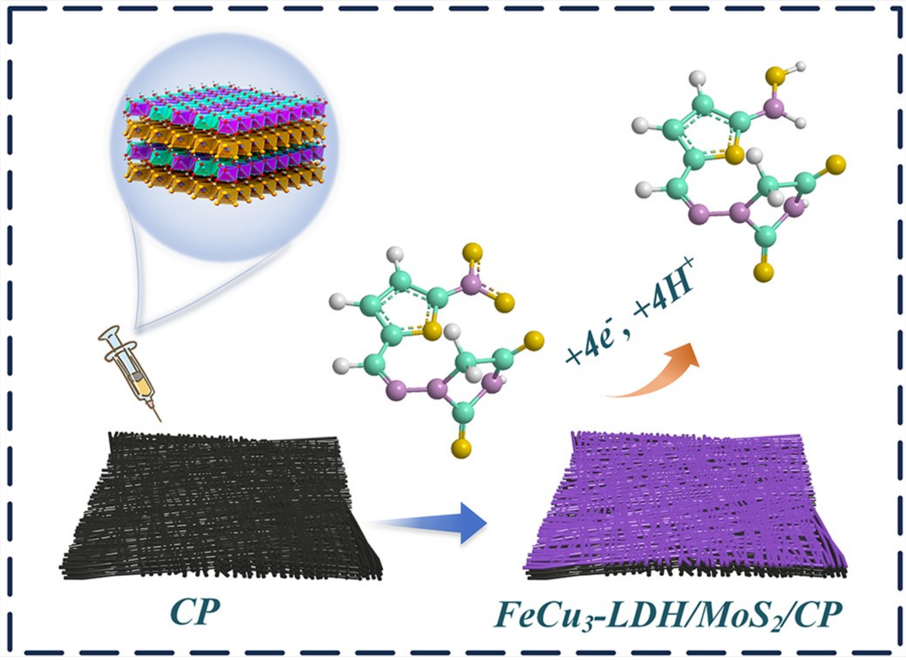

Fig. S7. Schematic diagram of the electrocatalysis mechanism of $FeCu_3$-LDH/MoS_2/CP (1:1) for NFT.

9. Condition optimization

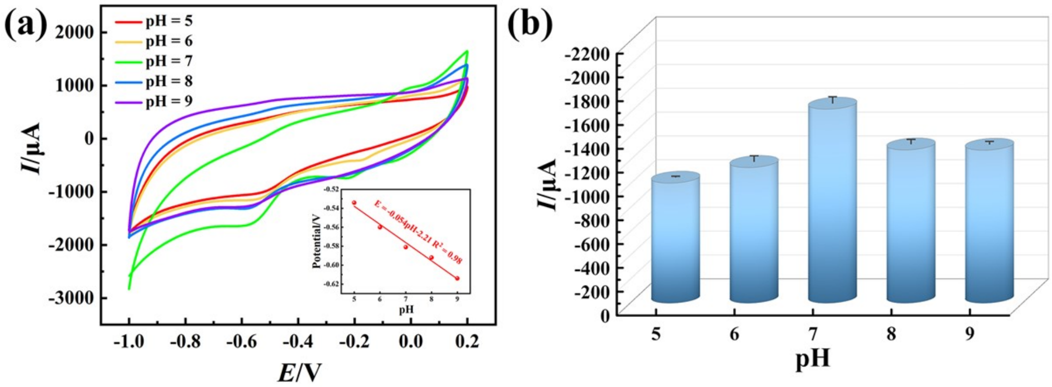

Fig. S8. (a) CV curves of FeCu$_3$-LDH/MoS$_2$/CP (1:1) at different pH in the presence of 50 μM NFT at scan rates of 100 mV·s^{-1}. Inset: relationship about pH and peak potential; (b) FeCu$_3$-LDH/MoS$_2$/CP (1:1) reduction peak current at different pH.

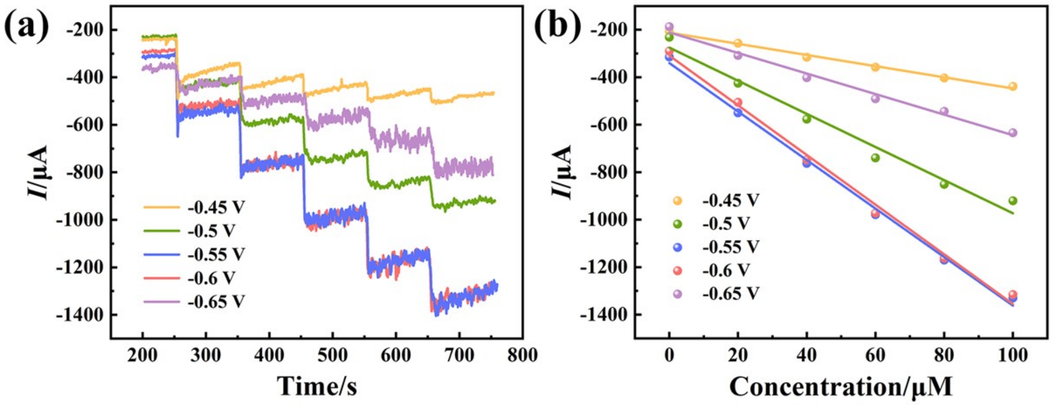

Fig. S9. (a) The i-t curves of $FeCu_3$-LDH/MoS_2/CP (1:1) at different test potentials; (b) Linear fitting plots of Ip vs. NFT concentrations at each test potential.

10. selectivity

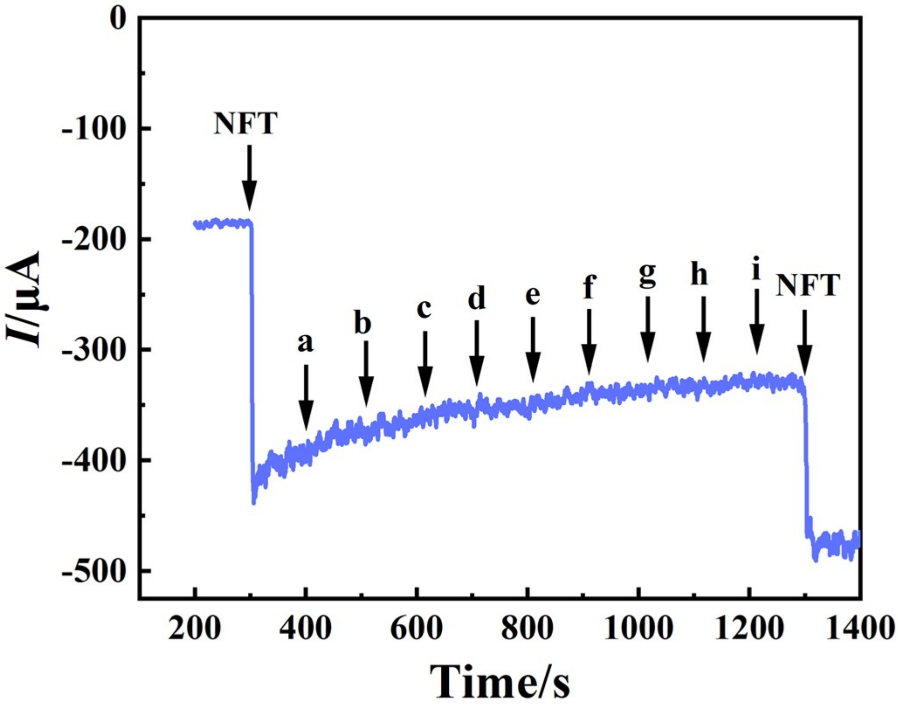

Fig. S10. The selectivity of $FeCu_3$-LDH/MoS_2 (1:1) in the presence of 20 μM NFT.

11. Test stability

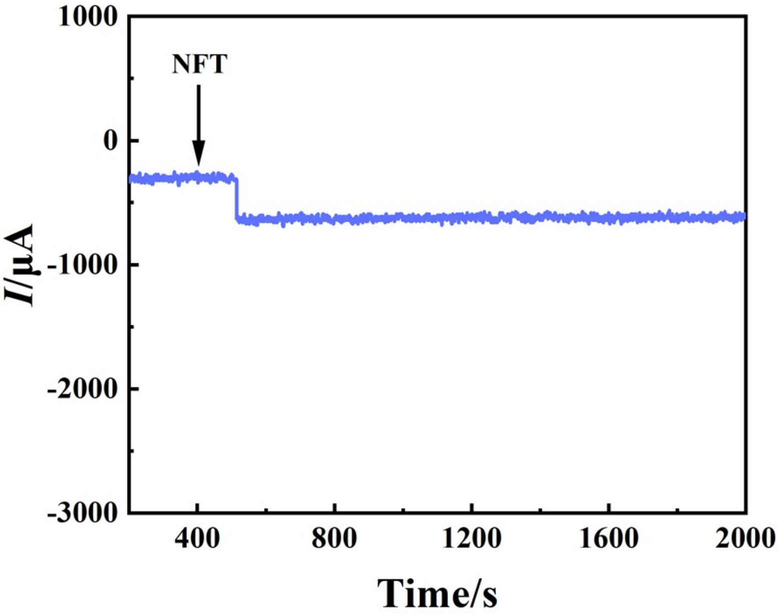

Fig. S11. The test stability of $FeCu_3$-LDH/MoS_2/CP (1:1) in the presence of 50 μM NFT.

12. Impedance fitting data for different materials

Table S1. Impedance fitting data for different electrodes

Electrode	R_s/Ω	$C_{dl}/\mu F$	R_{ct}/Ω	$Z_w/(\Omega \cdot cm^{-2})$
$FeCu_3$-LDH/MoS_2/CP (1:1)	7.89	1.504×10^{-4}	4.32	2026.5
$FeCu_3$-LDH/MoS_2/CP (1:4)	8.96	1.623×10^{-4}	5.28	3743.3
$FeCu_3$-LDH/MoS_2/CP (4:1)	11.19	2.536×10^{-4}	10.23	2619.2

13. Real sample detection

Table S2. The determination results and recovery of NFT in serum and lake water (n = 3)

Sample	Added/μM	Found (μM)	Recovery (%)	RSD (%)
Serum	1.0	0.98	98.00%	3.76%
	1.0	0.95	95.00%	
	1.0	1.14	101.40%	
	10.0	10.06	100.60%	3.04%
	10.0	9.93	99.30%	
	10.0	10.42	104.20%	
	20.0	20.37	101.80%	4.25%
	20.0	20.14	100.70%	
	20.0	19.86	99.30%	
Lake water	1.0	0.95	95.00%	4.55%
	1.0	1.08	108.00%	
	1.0	0.98	98.00%	
	10.0	9.88	98.80%	3.15%
	10.0	9.96	99.60%	
	10.0	10.23	102.30%	
	20.0	19.80	99.00%	3.34%
	20.0	20.20	101.00%	
	20.0	20.08	100.4.00%	

14. Determination of NFT in nitrofurantoin enteric-coated tablets

Table S3. Determination of NFT in nitrofurantoin enteric-coated tablets (n = 3)

Sample	Content (mg/tablet)	Measured content(mg/tablet)	Average (mg/tablet)	Recovery (%)	RSD (%)
Nitrofurantoin enteric-coated tablets	50.00	48.88 49.56 50.23	49.56	97.76% 99.12% 100.46%	3.35%

References

[1] J. Qu, F. Li, M. Wang, S. Subakti, M. Deconinck, G. Chen, Y. Li, L. Liu, X. Wang, M. Yu, D. Wolf, A. Lubk, B. Büchner, Y. Vaynzof, O.G. Schmidt, F. Zhu, One-Pot Synthesis of Nitrate-Intercalated NiFe Layered Double Hydroxides with an 8.2 Å Interlayer Spacing, Advanced Materials Interfaces 9(25) (2022) 2200973.

[2] Z.W. Lu, J. Zhong, Y. Zhang, M.M. Sun, P. Zou, H.J. Du, X.X. Wang, H.B. Rao, Y. Y. Wang, MOF-derived $Co_3O_4/FeCo_2O_4$ incorporated porous biomass carbon: simultaneous electrochemical determination of dopamine, acetaminophen and xanthine, J. Alloys Compd. 858 (2021), 157701

[3] D. Mohapatra, N.S.K. Gowthaman, M.S. Sayed, J.J. Shim, Simultaneous ultrasensitive determination of dihydroxybenzene isomers using GC electrodes modified with nitrogen-doped carbon nano-onions, Sens. Actuators, B 304 (2020), 127325.